Psychopharmacology (2011) 213:377–391
DOI 10.1007/s00213-010-2041-2

ORIGINAL INVESTIGATION

Ultrastructural characterization of tryptophan hydroxylase 2-specific cortical serotonergic fibers and dorsal raphe neuronal cell bodies after MDMA treatment in rat

Csaba Ádori · Péter Lőw · Rómeó D. Andó · Lise Gutknecht · Dorottya Pap · Ferencné Truszka · József Takács · Gábor G. Kovács · Klaus-Peter Lesch · György Bagdy

Received: 15 June 2010 / Accepted: 29 September 2010 / Published online: 30 October 2010

Abstract
Rationale 3,4-Methylenedioxymethamphetamine (MDMA, "ecstasy") is a widely used recreational drug known to cause selective long-term serotonergic damage.
Objectives The aim of this study was to characterize the ultrastructure of serotonergic pericarya and proximal neurites in the dorsal raphe nucleus as well as the ultrastructure of serotonergic axons in the frontal cortex of adolescent Dark Agouti rats 3 days after treatment with 15 mg/kg i.p. MDMA.
Methods Light microscopic immunohistochemistry and pre-embedding immunoelectron microscopy with a novel tryptophan hydroxylase-2 (Tph2) specific antibody, as a marker of serotonergic structures.

The high resolution version of the original images are available in the supplementary figures.

Electronic supplementary material The online version of this article (doi:10.1007/s00213-010-2041-2) contains supplementary material, which is available to authorized users.

C. Ádori · R. D. Andó · G. Bagdy (✉)
Department of Pharmacodynamics, Semmelweis University,
Nagyvárad tér 4,
1089 Budapest, Hungary
e-mail: bag13638@iif.hu

C. Ádori · D. Pap · G. Bagdy
Department of Pharmacology and Pharmacotherapy,
Semmelweis University,
Budapest 1089, Hungary

P. Lőw
Department of Anatomy, Cell and Developmental Biology,
Eötvös Loránd University of Sciences,
1117 Budapest, Hungary

R. D. Andó
Institute of Exptl. Medicine, Hungarian Acad. of Sci,
Budapest 1089, Hungary

L. Gutknecht · K.-P. Lesch
ADHD Clinical Research Network, Unit of Molecular Psychiatry,
Laboratory of Translational Neuroscience,
Department of Psychiatry, Psychosomatics, and Psychotherapy,
University of Wuerzburg,
97080 Wuerzburg, Germany

F. Truszka
1st Department of Pathology and Experimental Cancer Research,
Semmelweis University,
1085 Budapest, Hungary

J. Takács
Infobionic and Neurobiological Plasticity Research Group,
Hungarian Academy of Sciences—Peter Pazmany Catholic University—Semmelweis University,
1085 Budapest, Hungary

G. G. Kovács
Institute of Neurology, Medical University of Vienna,
Vienna 1097, Austria

G. Bagdy
Group of Neurochemistry Hungarian Academy of Sciences
and Semmelweis University Budapest,
1083 Budapest, Hungary

G. Bagdy
Group of Neuropsychopharmacology,
Hungarian Academy of Sciences
and Semmelweis University Budapest,
1083 Budapest, Hungary

Results Light microscopic analysis showed reduced serotonergic axon density and aberrant swollen varicosities in the frontal cortex of MDMA-treated animals. According to the electron microscopic analysis, Tph2 exhibited diffuse cytoplasmic immunolocalization in dorsal raphe neuronal cell bodies. The ultrastructural-morphometric analysis of these cell bodies did not indicate pathological changes or significant alteration in the cross-sectional areal density of any examined organelles. Proximal serotonergic neurites in the dorsal raphe exhibited no ultrastructural alteration. However, in the frontal cortex among intact fibers, numerous serotonergic axons with destructed microtubules were found. Most of their mitochondria were intact, albeit some injured axons also contained degenerating mitochondria; moreover, a few of them comprised confluent membrane whorls only.

Conclusions Our treatment protocol does not lead to ultrastructural alteration in the serotonergic dorsal raphe cell bodies and in their proximal neurites but causes impairment in cortical serotonergic axons. In these, the main ultrastructural alteration is the destruction of microtubules although a smaller portion of these axons probably undergo an irreversible damage.

Keywords 3,4-methylenedioxymethamphetamine (MDMA, "Ecstasy") · Serotonin (5-HT) · Microtubule · Degeneration · Morphometry · Tryptophan hydroxylase-2 (Tph2) · Pre-embedding immunoelectron microscopy

Introduction

The synthetic ring-substituted amphetamine derivate 3,4-methylenedioxymethamphetamine (MDMA, "Ecstasy") is a popular psychoactive recreational substance with entactogenic effect (Capela et al. 2009; Green et al. 2003). Regular use of MDMA may lead to acute and long-term cognitive and psychiatric problems (Green et al. 2003). In addition, MDMA-related medical complications have risen more than 20-fold in recent years (Puerta et al. 2009). The acute behavioral effects of MDMA are associated with the release of monoamines from nerve endings in the brain (Green et al. 2003).

MDMA administration causes long-term decrease in numerous serotonergic parameters such as long-term depletion in serotonin (5-HT, 5-hydroxytryptamine) concentration, reduction in the major 5-HT metabolite 5-hydroxyindoleacetic acid, loss of serotonin uptake and uptake sites as well as inhibition of tryptophan hydroxylase (Tph) activity in the forebrain of rats, guinea pigs, and primates (Green et al. 2003; Molliver et al. 1990). Several studies interpret the persistent decrease of serotonergic parameters as the consequence of physical destruction and disappearance of serotonergic axons (distal axotomy) (Molliver et al. 1990; Ricaurte et al. 1988). However, early studies have already noted that changes in 5-HT metabolic activity can precede—and may occur independently of—the processes determining degeneration of serotonergic axons and terminals (Battaglia et al. 1988). Taken together, it is still controversial whether the frequently used term "serotonergic neurotoxicity" related to MDMA implicates persistent neuroadaptive response of serotonergic markers or physical damage of serotonergic fibers, or as raised by Wang and coworkers, the combination of the two mechanisms (Kivell et al. 2010; Meyer et al. 2008; Wang et al. 2007).

To further elucidate this problem, we have used pre-embedding immuneoelectron microscopy, a method that has not been used in the examination of MDMA neurotoxicity in case of rat models yet. Fornai et al. (2004) have described multi-layer ubiquitin and Hsp70 immunoreactive (IR) nuclear and cytoplasmic membrane whorls in the nigral and striatal neurons of MDMA-treated mice. However, in mice, MDMA induces serious dopaminergic neurotoxicity unlike in rats and primates (Fornai et al. 2005), which might explain the nigrostriatal damage.

Here we labeled serotonergic neuronal elements with an antibody raised against the brain isoform of tryptohphan hydroxylase (Tph2) and we examined the light microscopic appearance as well as ultrastructural integrity of labeled dorsal raphe neuronal cell bodies and frontal cortex axons. We applied a single 15 mg/kg intraperitoneal MDMA treatment in adolescent male Dark Agouti rats. This treatment protocol and similar models of MDMA neurotoxicity have already been characterized extensively in many aspects by our group and others (Ando et al. 2010; Balogh et al. 2004; Kirilly et al. 2008; Kovacs et al. 2007; O'Shea et al. 1998; Quate et al. 2004).

The present study, together with previous data from the literature, may provide significant new information about the morphological basis of the potential serotonergic system damage caused by MDMA.

Material and methods

Animals

All animal experiments and housing conditions were carried out in accordance with the European Community Council Directive of 24 November 1986 (86/609/EEC) and the National Institutes of Health "Principles of Laboratory Animal Care" (NIH Publications No. 85–23, revised 1985), as well as specific national laws (the Hungarian Governmental Regulation on animal studies, 31 December

1998 Act). Permission was obtained from local ethical committees.

Male Dark Agouti rats (Harlan, Olac Ltd, Shaw's Farm, Blackthorn, Bicester, Oxon, UK, 5 weeks old upon arrival) were used in the experiments. The animals (three per cage) were kept under controlled environmental conditions (temperature at 21±1°C, and a 12-h light–dark cycle starting at 6:00 A.M.). Standard food and water were freely available.

Drug administration and treatment protocol

±3,4-methylenedioxymethamphetamine hydrochloride (MDMA, certified reference compound, purity >99.5%) was provided by Sanofi-Synthelabo-Chinoin, Hungary. The drug was dissolved in 0.9% NaCl at doses equivalent to 15 mg/kg free base and was injected intraperitoneally in a volume of 1 ml/kg into 7-week-old animals (MDMA group). Control animals received injections of 0.9% NaCl in a volume of 1 ml/kg at their age of 7 week (saline group). Rats were perfused 3 days after the MDMA/saline treatment.

Light microscopic immunohistochemistry and densitometric analysis of Tph2 IR cortical fibers

The rats (n=5 and 7, control and MDMA-treated groups, respectively) were anesthetized with pentobarbital-sodium (Nembutal; CEVA-Phylaxia, Hungary; 35 mg/kg, i.p.), thoracotomized, and perfused transcardially with Zamboni's fixative (Adori et al. 2006). The brains were removed and postfixed overnight at 4°C in the same solution and were embedded into paraffin. Coronal sections were cut on the levels of the striatum, hippocampus, and dorsal-median raphe following a conventional rat brain atlas (Paxinos 1986). The 5-μm sections were collected on silane-coated glass slides. One series of sections was stained for Luxol fast blue/Cresyl Violet staining.

For immunohistochemistry, after blocking the endogenous peroxidase activity with 0.03% hydrogen-peroxide (DAKO, Glostrup, Denmark), sections were incubated for 30 min at room temperature in 3% non-fat dry milk in PBS (pH 7.4) and for 2 h with primary antibodies (rabbit polyclonal anti-Tph1 and Tph2, diluted 1:5,000). Both antibodies were prepared according to the same protocol. The full description and characterization of antibodies have been described before (Gutknecht et al. 2009; Gutknecht et al. 2008). Immunostaining was developed using a peroxidase/DAB kit (EnVision ™, DAKO, Glostrup, Denmark). Routine immunohistochemical controls included the omission of the primary antibody and incubation with pre-immune serum. All sections were covered with VectaMount mounting medium (Vector Laboratories Inc., Burlingame, CA, USA).

Densitometric analysis of Tph2 immunostaining was performed on the II–V layer of frontal cortex as described before (Adori et al. 2006).

Pre-embedding immunogold electron microscopy of Tph1 and Tph2

The rats (n=3, either of MDMA or control groups) were anesthetized with pentobarbital-sodium (Nembutal; CEVA-Phylaxia, Hungary; 35 mg/kg, i.p.), thoracotomized, and perfused transcardially with 200-ml oxygenated Tyrode's solution (0.8% NaCl, 0.02% KCl, 0.1% $NaHCO_3$, 0.026% $CaCl_2 \times 2H_2O$, 0.005% $NaH_2PO_4 \times 2H_2O$, 0.1% glucose; ice cold, oxygenized with carbogen, pH 7.4) then with 25 ml fixative containing 2% paraformaldehyde in 0.1 M Na-acetate buffer (pH 6.5) for 2 min, followed by 500 ml fixative containing 2% paraformaldehyde and 0.1% glutaraldehyde in 0.1 M borate buffer (pH 8.5) for 1 h. After perfusion, the brains were left in skull overnight at 4°C for postfixation and then the removed brains were stored in 0.1 M PB (pH 7.4) pending analysis. Frontal vibratome sections (50-μm thick) were cut on the levels of both the striatum (between bregma +1.00 and +0.50) and dorsal-median raphe (−7.5 to −8.00) following a conventional rat-brain atlas (Paxinos 1986).

After washing in PB, sections were immersed in 1% sodium-borohydride in PB for 15 min and then were placed into PB containing 15% sucrose for 1 h and subsequently in PB containing 30% sucrose overnight at 4°C for cryoprotection. Then, sections were freezed–thawed three times by using liquid nitrogen to enhance antibody penetration. After extensive washing in PB and subsequently in TBS (pH 8.00), sections were incubated in 5% normal goat serum (NGS) in TBS for 3 h at 4°C (to block the nonspecific binding of antibodies) then in 2% NGS in TBS containing primary antibodies (rabbit polyclonal anti-Tph1 and anti-Tph2 antibodies, diluted 1:1,500; the two antibodies were employed separately) for 72 h at 4°C. Following extensive washing in TBS, sections were incubated in TBS containing 1% bovine serum albumin (BSA), 0.1% cold water fish-skin gelatin, and 0.1% sodium-azide (blocking solution with gelatin) for 30 min to inhibit nonspecific binding of gold probes to certain proteins. Then, sections were incubated in 0.8-nm gold-conjugated goat anti-rabbit immunoglobulin (Aurion, Ultra.Small immunogold reagents, Wageningen, The Netherlands; diluted 1:50 in blocking solution with gelatin overnight at 4°C). After extensive washing in both blocking solution with gelatin and in TBS, sections were postfixed in 1% glutaraldehyde in TBS for 10 min, washed in TBS and finally in Enhancement Conditioning Solution (ECS, Aurion). Silver intensification of the 0.8-nm gold particles was carried out using the Aurion R-Gent SE-LM reagent kit

for 5–10 min at 24°C. The enhancement was stopped by placing the section into ice-cold ECS solution.

After rinsing in PB, sections were osmicated in ice-cold 0.5% OsO_4 in PB for 15 min. Sections were washed in PB and distilled water, contrasted in 1% uranyl-acetate for 25 min, dehydrated in graded ethanol and finally in acetonitrile, and embedded in Durcupan (Fluca, Buchs, Switzerland) by flat-embedding between a glass microscope slide and glass coverslip which have been pretreated with liquid release agent (Electron Microscopy Science, Switzerland). The immunogold reactivity was checked under light microscope in the Durcupan-embedded sections. Selected areas of sections, including the II–IV layer of frontal cortex and the dorsal raphe nucleus, showing immunoreactivity for Tph2 were re-embedded in Durcupan blocks and serial sections were cut on ultramicrotome (LKB-II). Ultrathin sections (80–90-nm thick) were mounted on Formvar-coated 150-mesh or single-slot copper grids and were slightly counterstained with lead-citrate prior to ultrastructural analysis in a JEM-100CX II electron microscope (Jeol, Tokyo, Japan) operating at 60 kV.

Morphometric analysis of Tph2 IR dorsal raphe neurons and cortical fibers on electron microscopic sections

Ultrathin sections containing Tph2 IR dorsal raphe cell bodies were mounted on Formvar-coated single-slot grids. Two grids with a series of ultrathin sections were prepared from each block. Three blocks derived from three different flat-embedded 50-μm vibratome sections were applied from each animal. Before electron microscopic analysis, distribution of labeled cells was determined in parallel semithin sections. Micrographs were taken from an average of 2–4 Tph2 IR cell bodies with nucleus per block at the magnification of ×6,700. The high-resolution digitalized images (1,200 dpi) from each labeled cell bodies were merged and the sharpness and contrast were adjusted by Adobe® Photoshop® 7.0. The area of mitochondria, Golgi network, autophagic vacuoles, matured lysosomes, and multivesicular bodies (Figs. 4b–d, 5b) was measured and their cross-sectional areal density (micrometer-squared organelle per 100 μm^2 cytoplasm, %) or the density of somatic synapses (number of synapses per 100-μm cell membrane) were determined by two independent observers on the merged micrographs of 32 Tph2-immunostained dorsal raphe cell bodies from control and on 21 labeled dorsal raphe cell bodies from MDMA-treated animals (Figs. 4a, 5a) using ImageJ 1.37v software (NIH, USA, http://rsb.info.nih.gov/ij). The average cytoplasmatic area of the estimated cells were 103.5± 6.65 μm^2 or 105.3±8.17 μm^2, MDMA-treated and saline controls, respectively.

Ultrathin sections containing Tph2 IR cortical fibers were mounted on formvar-coated 150-mesh grids. Two grids with a series of ultrathin sections were prepared from each cortical block (layer II-IV). Two–three blocks derived from two–three different flat-embedded 50-μm vibratome sections were applied from each animal. A total of 321 and 442 Tph2 IR fibers were determined on control and MDMA-treated animals, respectively, according to a blind protocol at the magnification of ×40,000. These fibers were divided into two categories, namely, (1) fibers with intact microtubules and (2) fibers with destructed microtubular system (Fig. 6a vs. b; Fig. 8a–d vs. e–g).

Data obtained from morphometric analysis of labeled raphe cell bodies and cortical fibers were evaluated by Mann–Whitney *U* test with acceptable levels of significance set at $P<0.05$ using Statistica® 7 software. Figures 3 and 7 were prepared by GraphPad Prism® 4.00 software.

Results

Specificity of antibodies

In light microscopic sections, in addition to the widespread axonal immunostaining (Figs. 1e, 2a), rabbit polyclonal Tph2 antibody stained only raphe nuclei and some other neuronal pericarya of the brainstem corresponding anatomically to the serotonergic neuronal populations (Fig. 1a–b). In contrast, neither cell bodies nor fibers were immunoreactive for rabbit polyclonal Tph1 antibody in the brainstem (Fig. 1c) although pineal gland exhibited strong Tph1 immunostaining (Fig. 1c–d).

In the electron-microscopic sections, sparse granules of silver-gold labeling were detected in some neuronal nuclei omitting the first antibody. Very sparse granules of silver-gold labeling could be found in the dorsal raphe cell bodies or in the frontal cortex fibers either with intact or destructed microtubules in case of Tph1 immunostaining (data not shown).

Light microscopic analysis of Tph2 IR fibers after MDMA treatment

Three days after the single 15 mg/kg administration of MDMA, 35% reduction of Tph2-immunoreactive axon density was found in the frontal cortex (Figs. 2a–c, 3). In addition, numerous aberrant swollen varicosities could be detected in the frontal cortical sections after MDMA in contrast to the control animals (Fig. 2b–c and e, arrows). At higher magnification, Tph2 fiber immunoreactivity in the frontal cortex often exhibited fragmented and bulbous profile with large (2–4-μm in diameter) swollen varicosities

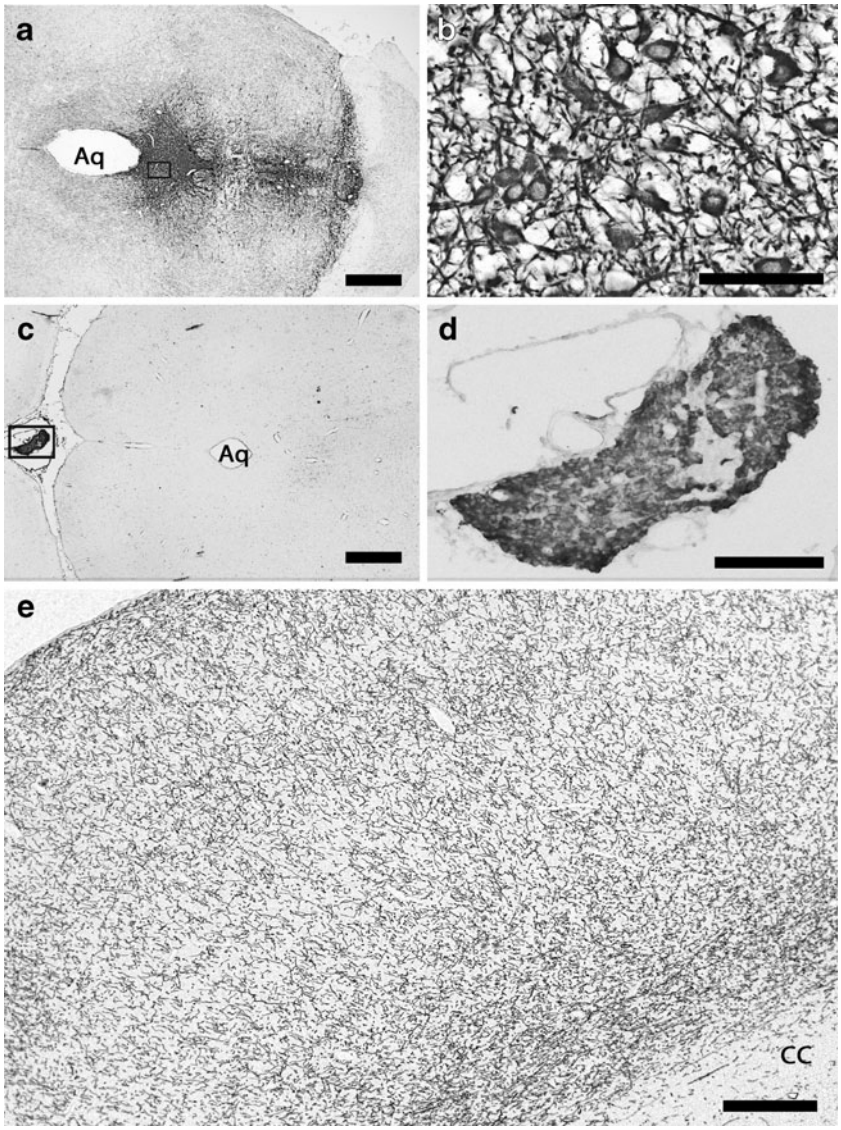

Fig. 1 Specificity of Tph1 and Tph2 rabbit polyclonal antibodies. Tph2 immunostaining in the dorsal/median raphe neurons and in fibers around them (**a**); Tph2 immunostaining in the dorsal raphe neurons (**b**). No cell bodies or fibers are immunoreactive for Tph1 in the brainstem (**c**). In contrast, pineal gland exhibits a strong Tph1-immunoreactivity (**c**, **d**). Tph2-immunoreactive fiber arborization in control frontoparietal cortex (**e**). Higher magnifications of the *boxed zones* in panels **a** and **c** are shown in panels **b** and **d**, respectively. *Scale bars*: 500 μm in panel **a** and **c**, 50 μm in panel **b**, 100 μm in panel **d**, 200 μm in panel **e**. *Aq* aqueduct, *CC* corpus callosum

in the treated animals. No such aberrant staining patterns were found in the control animals (Fig. 2e vs. d, MDMA-treated vs. control).

Electron microscopic analysis of Tph2 IR dorsal raphe neuronal cell bodies and proximal neurites

Tph2 exhibited diffuse cytoplasmic immunolocalization in many dorsal raphe cell bodies with no apparent association with any organelles (Figs. 4 and 5). The labeled dorsal raphe neurons were found to be morphologically heterogenic: fusiform, triangular, or multipolar cells with an average diameter of 10–20 μm. The nucleus was located centrally in the cytoplasm and was often indented. The ultrastructural-morphometric analysis of cell bodies did not indicate pathological changes (e.g., swollen mitochondria, protein inclusions, large membrane whorls) or significant alterations in the surface area of mitochondria, the Golgi network, components of the endosomal–lysosomal compartment (multivesicular bodies, mature lysosomes, autophagic structures) and in the number of somatic synapses in MDMA-treated animals compared to saline controls. A moderate increase was only noted in the surface area of matured lysosomes in the MDMA-treated group compared to saline control (P=0.08; Figs. 4b–d, 5b; Table 1).

Proximal serotonergic neurites in the dorsal raphe nucleus exhibited no ultrastructural alteration in the MDMA-treated animals compared to control (Fig. 6c–d).

Electron microscopic analysis of Tph2 IR cortical fibers

In the frontal cortical samples, silver-gold granules representing Tph2 immunolabeling were notably fewer than those in neurites or cell bodies in the dorsal raphe (Fig. 6a vs. c). Labeled axons with microtubules, mitochondria,

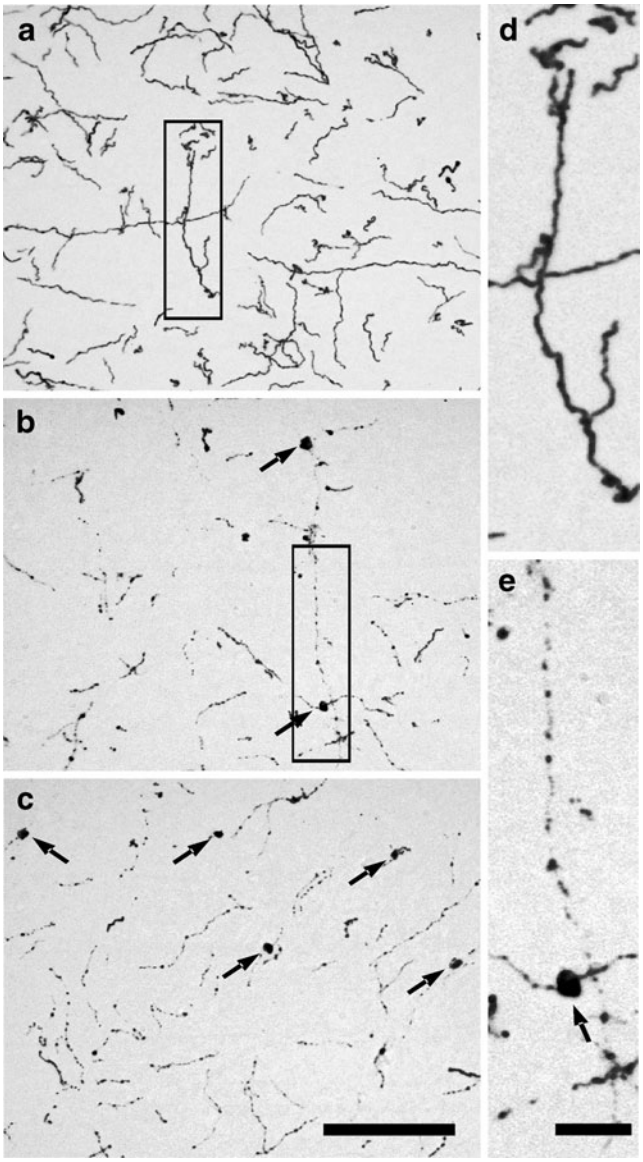

Fig. 2 Light microscopic analysis of Tph2 IR fibers after MDMA treatment. Tph2 IR axon arborization in the frontal cortex of a control animal is demonstrated in panel **a**. Reduced axon density and aberrant swollen varicosities (*arrows*) in the frontal cortex of MDMA-treated animals (**b**, **c**). Higher magnification of the *boxed zones* in panels **a** and **b** are shown in panels **d** and **e**, respectively. *Scale bars*: 25 μm in panel **c** applied to panels **a**–**c**; 5 μm in panel **e**, applied to panels **d**–**e**

SER tubules were detected in all around the examined areas with a slightly enhanced density around capillaries (Figs. 6a, 9a). Labeled axonal cross-sections were typically round- or ovoid-shaped, approximately 0.5–1.4 μm in diameter, containing microtubules, 1–2 mitochondria, and clear vesicles, but exhibiting only a few synapses (Fig. 8a–d). All labeled fibers were unmyelinated and no immunolabeled myelinated fiber was detected (Fig. 6a).

In the MDMA-treated animals, among Tph2-labeled fiber sections with morphologically intact microtubules, many labeled fibers with destructed microtubular system were observed. In these axons, microtubules were disorganized, fragmented, or completely disappeared (Fig. 8e–g). In some cases, aggregated microtubular elements with irregular shape were also noted (Fig. 6b). Axons with disrupted microtubular system were typical and their number was significantly higher in the MDMA-treated animals compared to controls (16% vs. 61%, saline vs. MDMA, $P<0.01$; Figs. 6a and 8a–d vs. 6b and 8e–g; Fig. 7). The distribution of axonal sections with damaged microtubules was homogenous in the samples examined and these structures occurred in all examined animals in a nearly similar amount (57–64%).

In the MDMA-treated animals, many of the labeled fibers with destructed microtubular system were swollen (Fig. 9c–d), contained membrane whorls, accumulated fragmented SER tubules/aberrant tubulovesicular structures, although their mitochondria were seemingly intact (Figs. 6b, 9b). In some axons, higher amount of dark mitochondria was found (Figs. 8g, 9d). Some injured axons also contained degenerating mitochondria (Fig. 9c–d), moreover, a few of them comprised confluent membrane whorls only (Fig. 9e). At the same time, no shrunken or dark processes were noted at all.

The described alterations were restricted principally to Tph2-labeled processes (Fig. 9b–c) and were not observed in cortical neuronal cell bodies or in glial elements. Non-labeled myelinated fibers were preserved (Fig. 8f).

Discussion

Specificity of Tph2 immunoreactivity and methodological considerations

In order to examine the morphological aspects of MDMA-induced neurotoxicity in more details, we applied light

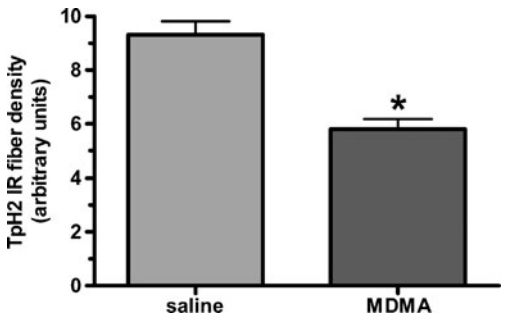

Fig. 3 Quantitative evaluation of Tph2 IR fiber density in the frontal cortex 3 days after MDMA treatment and saline control. The quantitative evaluation demonstrates the significantly reduced density of Tph2 IR fibers in the MDMA-treated group compared to the saline control. Statistical analysis: Student's *t* test for independent samples ($n=5$ and 7, saline and MDMA-treated groups, respectively, $P<0.05$)

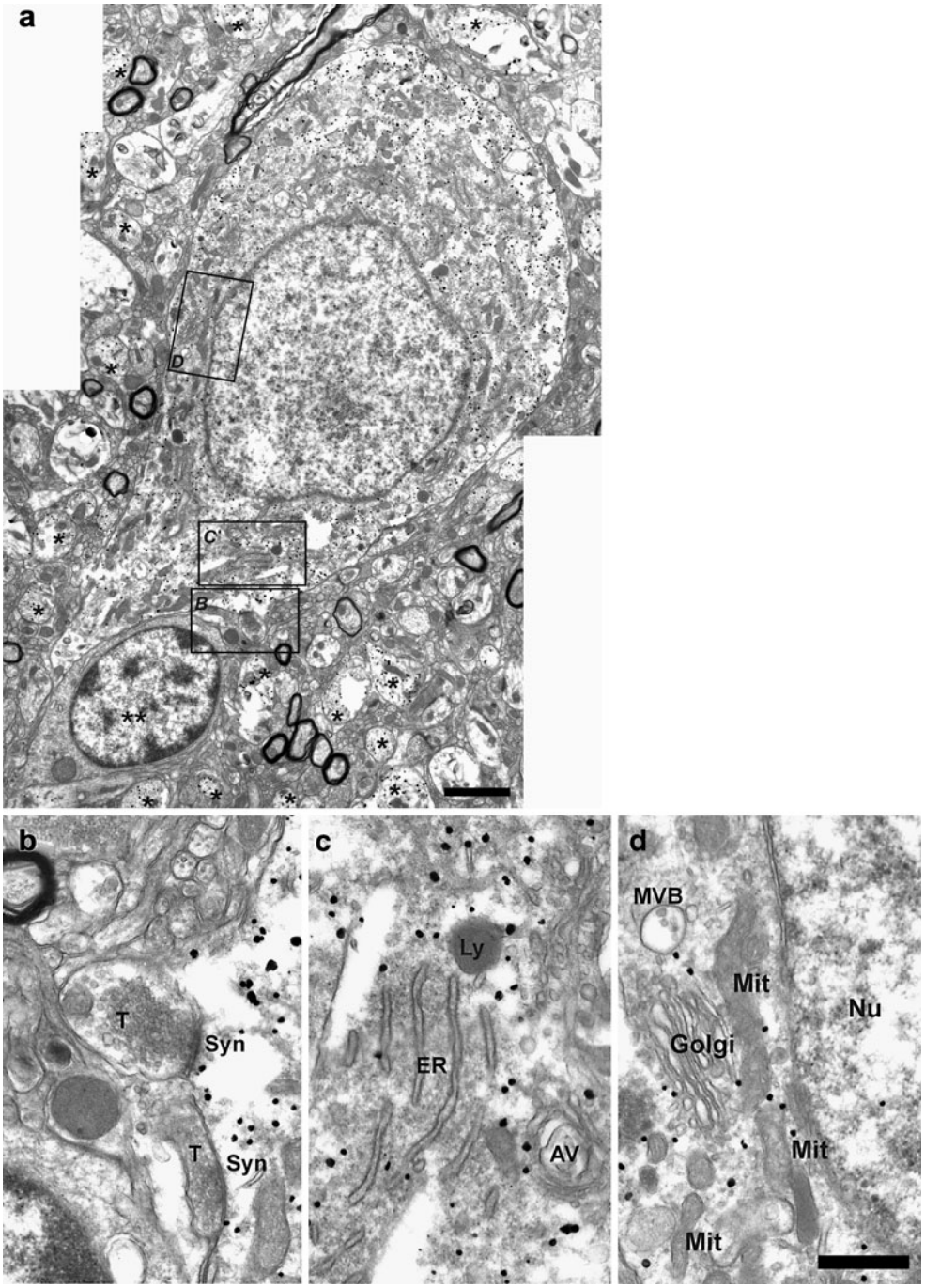

Fig. 4 Ultrastructural overview of a Tph2 immunolabeled dorsal raphe neuron from a saline control Dark Agouti rat. Overview of a Tph2 immunolabeled neuron (**a**); higher magnifications of the *boxed zones* in panel **a** are shown in panels **b**–**d**. Panels **b**–**d** demonstrates organelles involved in morphometry analysis. *ER*, endoplasmic reticulum; *Ly*, mature lysosome; *AV*, autophagic vacuole; *Nu*, nucleus; *Golgi*, Golgi network; *MVB*, multivesicular body; *Mit*, mitochondrion; *Syn*, somatic synapse; *T*, synaptic terminal; *one asterisk* (*), proximal serotonergic neurites; *two asterisks* (**), non-serotonergic (glial) cell. *Scale bars*: 1.5 μm in panel **a** and 0.5 μm in panel **d**, applied to **b**–**d**. Note that the labeled dorsal raphe cell body does not exhibit pathological alterations

microscopic and immunoelectron microscopic analysis of dorsal raphe and frontal cortical samples of adolescent Dark Agouti rats 3 days after the single 15 mg/kg i.p. MDMA treatment. We used a fully characterized, new rabbit polyclonal antibody against the brain-specific isoform of tryptophan hydroxylase (Tph2) as a brain serotonergic marker (Gutknecht et al. 2009; Gutknecht et al. 2008). The light microscopic immunostaining pattern of Tph2 is in agreement with previous studies on Tph localization (Adori et al. 2006; Tork 1990; Weissmann et al. 1987). The lack of brain immunostaining with the rabbit polyclonal Tph1 antibody is also in agreement with other studies that report no or only very minimal expression of Tph1 in the brain (Gutknecht et al. 2009; Malek et al. 2005).

The ultrastructural morphology of both the Tph2-immunolabeled dorsal raphe neuronal cell bodies and cortical unmyelinated axon sections in control animals are concordant with the description of serotonergic cell bodies and cortical axons published in previous papers (Arai et al. 2002; Baker et al. 1990; Cohen et al. 1995; Holzel and

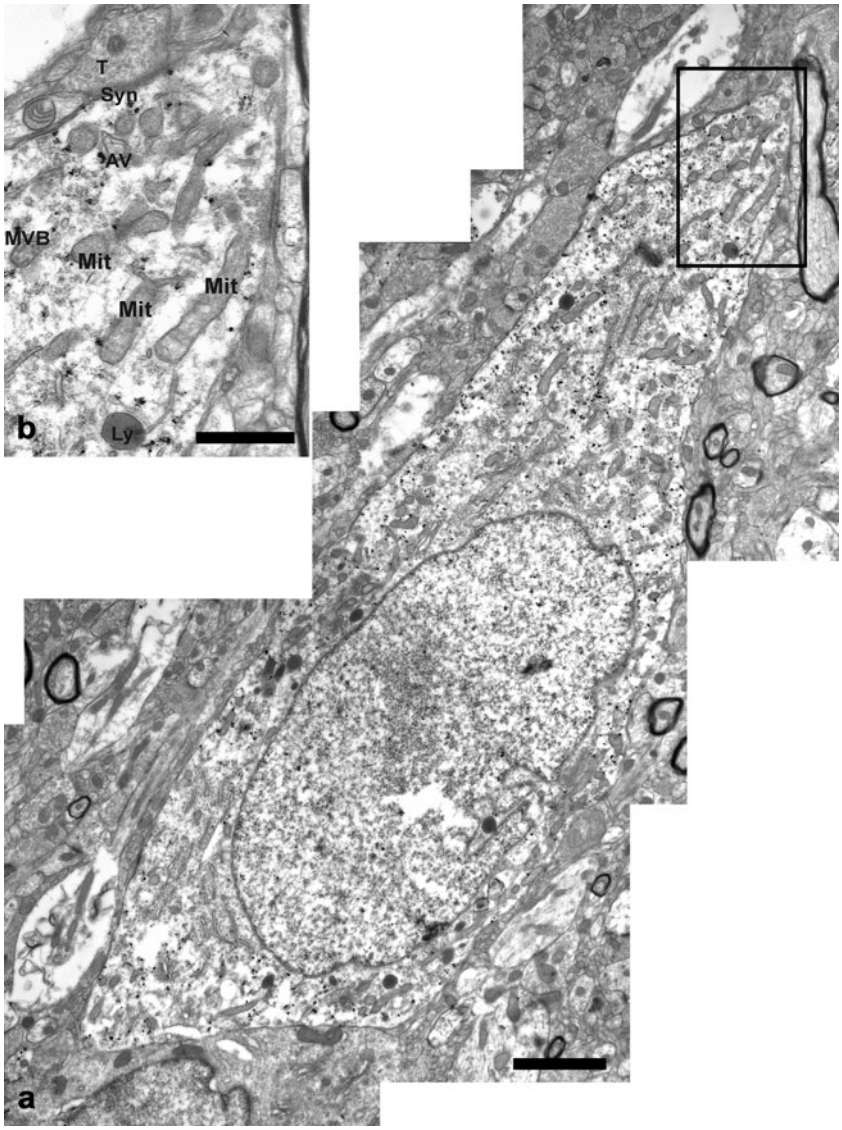

Fig. 5 Ultrastructural overview of a Tph2 immunolabeled dorsal raphe neuron from a MDMA-treated Dark Agouti rat. Overview of a Tph2 immunolabeled neuron (**a**); higher magnification of the *boxed zone* in panel **a** is shown in panel **b**. Panel **b** demonstrates organelles involved in morphometry analysis. *Ly*, mature lysosome; *AV*, autophagic vacuole; *MVB*, multivesicular body; *Mit*, mitochondrion; *Syn*, somatic synapse; *T*, synaptic terminal. *Scale bars*: 2 μm in panel **a** and 1 μm in panel **b**. Note that the labeled dorsal raphe cell body does not exhibit pathological alterations

Table 1 Cross-sectional areal density of organelles (micrometer-squared organelle per 100 μm^2 cytoplasm, %) or density of somatic synapses (number of synapses per 100-μm cell membrane) were evaluated on 21 Tph2-immunostained dorsal raphe cells from control and on 32 labeled dorsal raphe cells from MDMA-treated animals

Treatment	Organelle/structure						
	Mitochondria	Golgi	MVB	AV	Lysosome	MVB+AV+Lysosome	Synapse
Saline	6.44±0.32	6.92±0.55	0.35±0.05	0.39±0.09	0.93±0.1	1.66±0.13	13.27±1.32
MDMA	7.06±0.33	6.95±0.48	0.39±0.06	0.43±0.07	1.17±0.09[a]	1.99±0.12	14.07±0.91

Statistical analysis—Mann–Whitney *U* test, $P<0.05$

Data are expressed as±SEM

The ultrastructural–morphometrical analysis of cell bodies from treated animals did not indicate statistically significant alteration in the surface area of mitochondria, Golgi network (*Golgi*), components of the endosomal–lysosomal compartment (multivesicular bodies (*MVB*), mature lysosomes (*Lysosomes*), autophagic vacuoles (*AV*)), and in the number of somatic synapses

[a] $P=0.08$

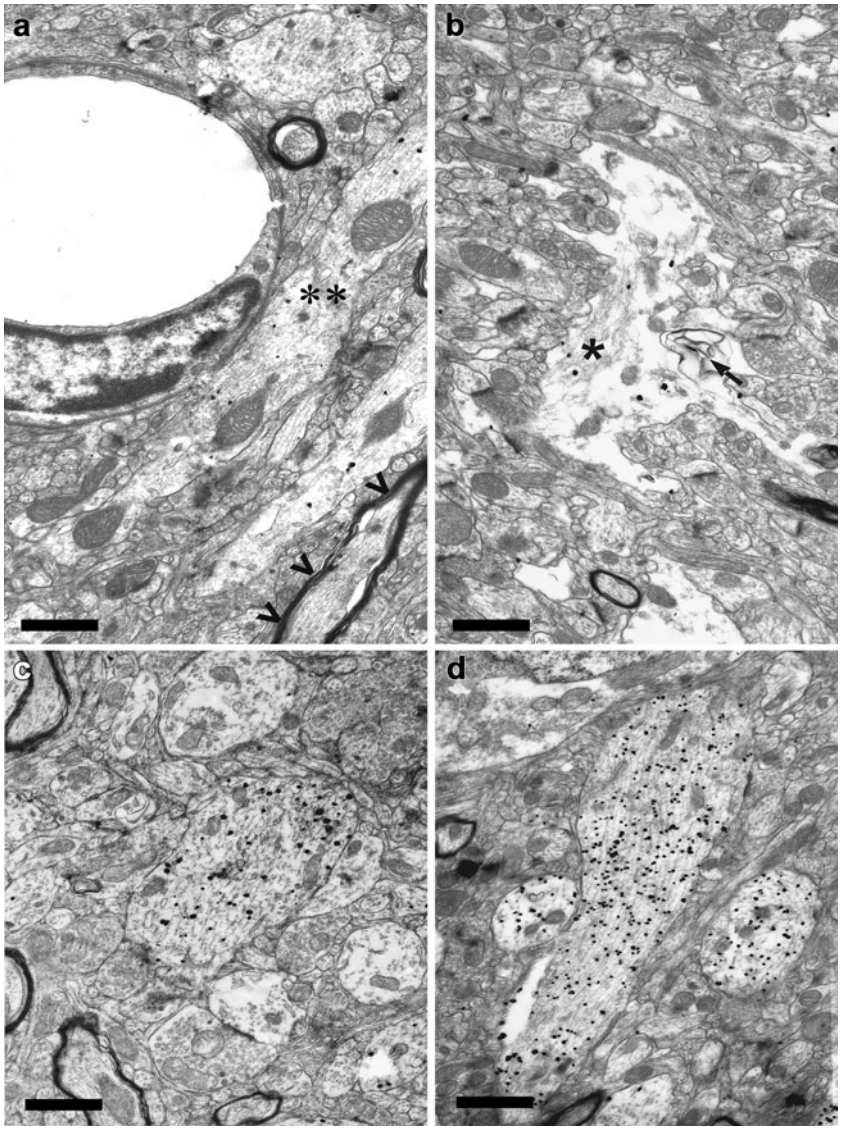

Fig. 6 Examples of Tph2 immunolabeled fibers from frontal cortex (**a–b**) and dorsal raphe (**c–d**) samples. Labeled fiber section with morphologically intact microtubular system near to a capillary from a control animal (**a**); labeled fiber section with destructed microtubular system from a MDMA-treated animal (**b**); labeled proximal neurites with morphologically intact microtubular system from a control and an MDMA-treated animal (panels **c** and **d**, respectively). Note the more intense immunolabeling of fibers in the neuropil of dorsal raphe sample (**c**, **d**) compared to the cortical fiber sections (**a**, **b**). *arrowhead* (<), myelinated non-serotonergic fiber section; *two asterisks* (**), labeled fiber section with morphologically intact microtubular system; *arrow* (↓), membrane whorl in labeled fiber section with disrupted microtubular system; *one asterisk* (*), disintegrated–aggregated microtubular elements. *Scale bars*: 1 μm in all panels

Pfister 1981; Liposits et al. 1985; Mori et al. 1987; Smiley and Goldman-Rakic 1996). Earlier studies on electron microscopic immunolocalization of Tph have reported some association of immunoreactivity with rough endoplasmic reticulum, Golgi membranes, and microtubules, besides the wide distribution of Tph IR in the cytoplasm (Joh et al. 1975; Pickel et al. 1976). However, our results on the diffuse cytoplasmic immunolocalization of Tph2 do not confirm it. This discrepancy may be related to the difference between visualization systems used (ABC technology and DAB precipitation in the studies of Joh and coworkers (Joh et al. 1975) and Pickel and associates (Pickel et al. 1976), a more precise nanogold labeling and silver intensification in our study). The less intense ultrastructural silver-gold immunolabeling, detected in the cortical fibers compared to dorsal raphe cell bodies and proximal serotonergic neurites, is in good agreement with light microscopic findings.

Our fixation procedure results in a generally well-preserved ultrastructure despite the immunolabeling procedure. Moreover, the nanogold silver-intensification technology let us to examine the detailed ultrastructure of serotonergic cells and fibers as the silver-gold particles only minimally masked the labeled structures.

Serotonergic neurotoxicity caused by MDMA

Following MDMA administration, long-lasting depletion of many serotonergic parameters can be detected and the time course of recovery coincides more closely with the time course of serotonergic axonal regeneration (sprouting; Callahan et al. 2001; Fischer et al. 1995). Secondly, the light microscopic analysis of serotonergic axons after MDMA revealed aberrant, swollen varicosities, and fragmented-like axonal morphology (Molliver et al. 1990; O'Hearn et al. 1988) that we can also confirm in this study

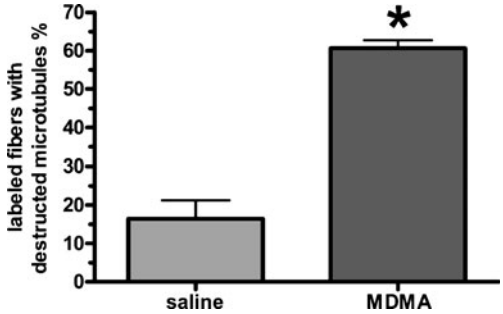

Fig. 7 Quantitative evaluation of Tph2-labeled fiber sections with morphologically intact microtubular system vs. damaged microtubules 3 days MDMA treatment. The quantitative evaluation demonstrates a significantly increased amount of Tph2 immunolabeled fiber sections with destructed microtubular system in the MDMA-treated group compared to the saline control. Statistical analysis: Mann–Whitney *U* test ($n=3$, in either MDMA or saline treated groups, $P<0.05$)

based on Tph2 immunohistochemistry. In addition, the long-term decrease (50%) in anterograde axonal transport of axons originating in the rostral raphe nuclei was detected 3 weeks after the drug treatment (Callahan et al. 2001). However, according to our previous results, amyloid precursor protein-IR axonal bulbs cannot be observed after MDMA treatment, which suggest that no complete blockage of fast axonal transport occurred (Kovacs et al. 2007; Medana and Esiri 2003). In a recent study, a significant reduction of both 5-HTT expression and protein level have been described in parallel with unaltered protein level of vesicular monoamine transporter 2 (VMAT2) 2 weeks after a binge MDMA treatment in rats (Biezonski and Meyer 2010). Finally, the glial reaction after MDMA is still a question of debate, many authors failed to detect reactive astrogliosis (increased glial fibrillary acidic protein (GFAP) immunoreactivity or protein level) after the treatment (O'Callaghan and Miller 1993; Wang et al. 2004). However, others argue that GFAP method is not sensitive enough to detect such a small lesion of axons as the putative degeneration of serotonergic axons after MDMA administration (Bendotti et al. 1994; Rowland et al. 1993). At the same time, we and others have described reactive astrogliosis in the hippocampus (Adori et al. 2006; Aguirre et al. 1999) and also microgliosis (Orio et al. 2004) in both the cortex and hypothalamus of rats, although these glial reactions do not necessarily reflect to axonal degeneration.

Effects of MDMA on the ultrastructure of dorsal raphe neuronal cell bodies

Ricaurte et al. described shrunken cell bodies and lipofuscin-like cytoplasmatic inclusions in the dorsal but not the median raphe of MDMA-treated monkeys (Ricaurte et al. 1988). In contrast, no evidence of altered morphology, picnosis, or cellular degeneration in dorsal raphe cell bodies or dendrites was detected in Nissl-preparation on frozen sections from MDMA-treated rats, although the authors emphasize that a more subtle morphological analysis is required in this field (O'Hearn et al. 1988). Our ultrastructural analysis of serotonergic dorsal raphe cell bodies is in concordance with the latter study in rats and indicates that there are no pathological alterations (swollen or picnotic mitochondria, membrane whorls, protein inclusions, etc.) in these cell bodies in treated animals compared to saline control.

As the actual total amount of certain organelles may reflect to the actual metabolic conditions of the cell (Welt et al. 2004), we have analyzed the surface density of mitochondria, Golgi network, autophagic vacuoles, matured lysosomes, and multivesicular bodies (Fader and Colombo 2009), as well as we have determined the number of perisomatic synapses in the serotonergic dorsal raphe cell bodies 3 days after the MDMA treatment and we did not found significant alterations. The only interesting observation was the trend toward increase (+26%) in the surface density of matured lysosomes that may reflect a slight increase of lysosomal degradation in these cells (Nixon and Cataldo 1995). Taken together, we can establish that 3 days after the treatment, MDMA does not cause metabolic alterations that would manifest in significant increase of the surface density of mitochondria, Golgi network, the endosomal–lysosomal compartment, and the number of somatic synapses (Morshedi et al. 2009) in serotonergic dorsal raphe cell bodies.

Microtubular injury after MDMA treatment

The most apparent alteration in the ultrastructure of the labeled cortical axons of MDMA-treated animals was the widespread disorganization or destruction of microtubular system, which was found in approximately 60% of all labeled fiber sections. This result is in good agreement with the finding that anterograde axonal transport in fibers originating in the rostral raphe nuclei was decreased after MDMA treatment (Callahan et al. 2001). Axonal microtubules support fast and slow axonal transport of cellular components both anterogradly and retrogradly (Baas and Qiang 2005; Tanner et al. 1998). Moreover, a tight correlation between cytoskeletal disintegration and the serious decrease in fast axonal transport has already been demonstrated in other experimental models earlier (De Repentigny et al. 2003; Sahenk and Mendell 1983). The morphological sign of microtubular destruction was noted in the control animals only rarely. This effect has been described by some ultrastructural studies and has been interpreted as a result of neural plasticity or certain fixation condition (Linder et al. 1995; Ryan et al. 1990). Taken together, ultrastructural analysis of serotonergic fibers in the frontal cortex suggests a widespread collapse of axonal

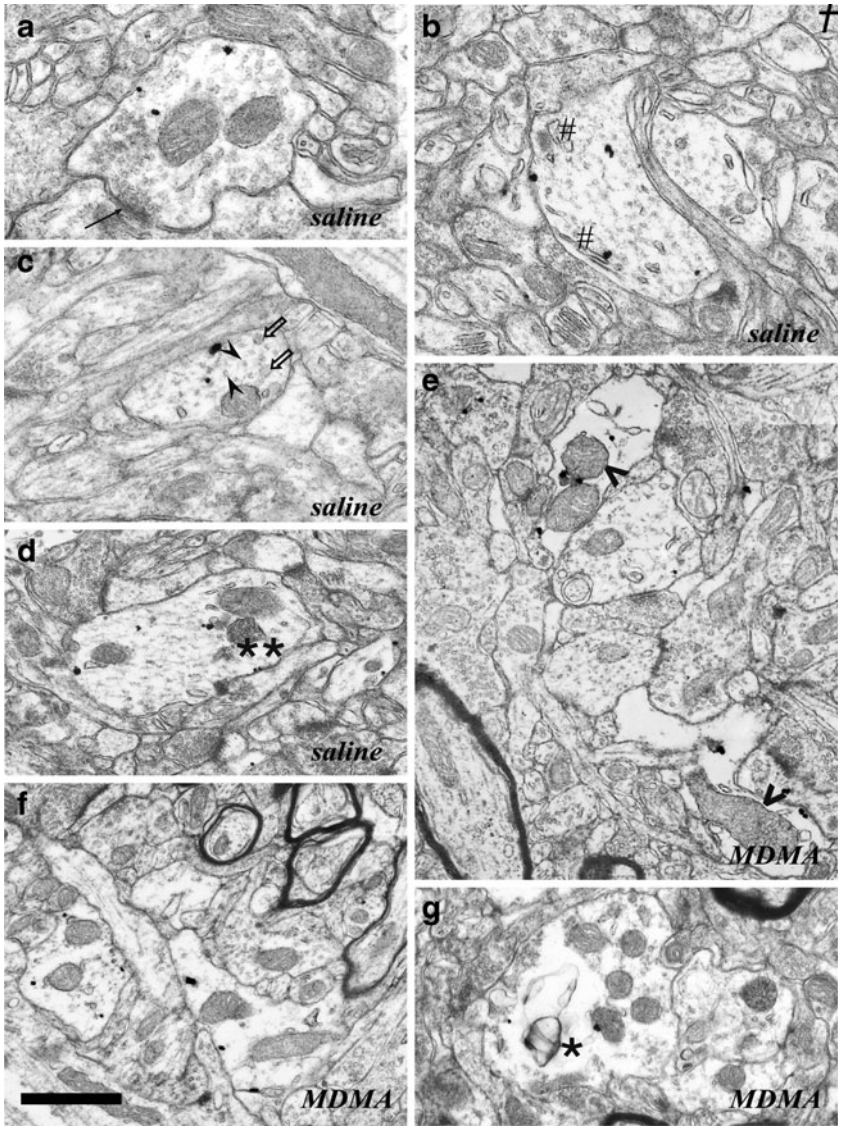

Fig. 8 Examples of Tph2 immunolabeled axons—axon terminals from frontal cortex of control (**a–d**) and MDMA-treated (**e–g**) animals I. Note the labeled axons with damaged microtubules but morphologically intact mitochondria in the treated animals (panel **e** vs. panels **a–d**). Labeled axons in the treated animals occasionally contained irregular membranous structures and a higher number of mitochondria (panel **g**). *Open arrow*, clear vesicles; *arrowheads*, cross-sections of microtubules; *number sign* (#), SER tubules; *one asterisk* (*), membrane whorl; *two asterisks* (**), multivesicular body; *arrow*, synapse; *arrowhead* (>), morphologically intact mitochondria. *Scale bar*: 0.5 μm in panel **f** applied to all panels

microtubular system after MDMA administration. Alternatively, it is also possible that MDMA treatment results in an enhanced instability of microtubules that makes them more vulnerable to fixation/embedding procedures. It is unclear, why certain axons exhibit the collapse of microtubular system after MDMA while others do not. One can speculate that the sensitivity of microtubules to the effects of MDMA may depend, at least partly, on microtubule-associated proteins (MAPs) and on other factors that influence the actual stability of microtubular system (Baas and Qiang 2005).

The disorganized/collapsed microtubular system leads to axonal swelling, fragmentation of SER vesicles, or even to the appearance of tubulovesicular structures or aggregated microtubular elements (Sahenk and Mendell 1983). These aberrant structures were common in our sections from MDMA-treated animals. At the same time, in these axons with microtubular injury, mitochondria were mostly intact.

The integrity of microtubular system is highly sensitive to oxidative stress (Baas and Qiang 2005; Bellomo et al. 1990), which has a prominent role in MDMA-caused neurotoxicity (Puerta et al. 2009). In addition, MDMA treatment alters the expression of activity-regulated cytoskeleton-associated protein, which may be a further effect of MDMA on stability of the cytoskeleton (Beveridge et al. 2004). At the same time, microtubular disorganization, destruction, cytoskeletal injury, and axonal swelling do not necessarily result in an irreversible degeneration and elimination of axons (Graham and Lantos 2002; Medana and Esiri 2003; Tanner et al. 1998).

The technical procedure of fixation, pre-embedding immunostaining, and embedding in our work do not allow us to examine the ultrastructure of neurofilaments, another important component of axonal cytoskeleton. Further studies are needed to determine the involvement of neurofilaments in MDMA-caused neurotoxicity.

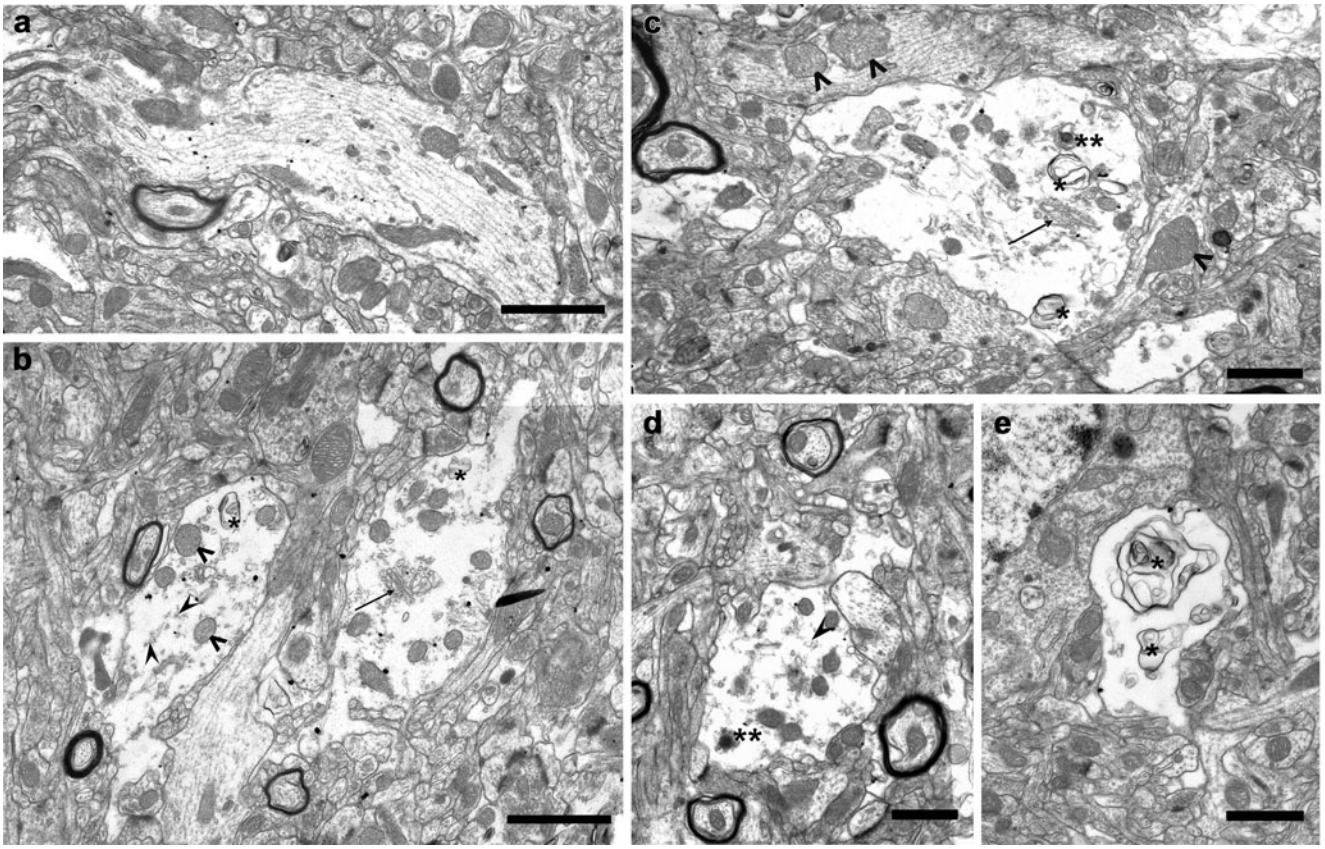

Fig. 9 Examples of Tph2 immunolabeled fibers from frontal cortex samples of control (**a**) and MDMA-treated (**b–e**) animals II. Horizontal section of a labeled fiber with morphologically intact microtubular system from a control animal (**a**); labeled axon with destroyed microtubules, membrane whorls, aggregated SER-elements but morphologically intact mitochondria (**b**); swollen labeled fibers with destructed microtubules, morphologically intact but often dark mitochondria, degenerating mitochondria, and membrane whorls (**c–d**); labeled fiber with confluent membrane whorls (**e**). *Arrowhead*, disintegrated cytoskeletal elements; *less than sign* (>), morphologically intact mitochondrion; *arrow*, aggregated SER-elements; *two asterisks* (**), degenerating mitochondrion; *one asterisk* (*), membrane whorl. *Scale bars*: 1 μm in all panels

More severe injury of serotonergic axons after MDMA treatment

In our study, besides serotonergic axons with collapsed microtubules but with intact mitochondria, some labeled axons also contained degenerated mitochondria and a minority of them comprised confluent membrane whorls only. Several previous studies have described similar fiber alterations in the rat brain after different drug treatments such as iminodipropionitrile (Chou and Hartmann 1964), n-butyl ketone (Spencer and Schaumburg 1975), 2,5-hexanedione (Sahenk and Mendell 1983), methamphetamine (Sharma and Kiyatkin 2009). Papers on the ultrastructural analysis of amphetamine treatment have identified two main types of degeneration: swollen processes either devoid of organelles or filled with membranous debris ("early stage") and dark profiles with often irregular outlines ("later stage"; Linder et al. 1995; Ryan et al. 1990). Essentially, similar categories have been established by Martinez et al. in a Wallerian-degeneration model (Marques et al. 2003; Narciso et al. 2001). They describe "watery degeneration" that starts with the focal disintegration of cytoskeleton followed by axonal swelling when the axoplasm is either replaced by an amorphous and granular material or completely devoid of organelles. In the second category, the cytoskeleton becomes aggregated and the authors suggest that this will probably turn the axoplasm progressively denser, characterizing the "dark form" of degeneration. In contrast to Ryan et al. (Ryan et al. 1990), Marques et al. (Marques et al. 2003) suggest that the two types of axon degenerations are parallel processes. The serotonergic fibers in our study with degenerated mitochondria and with confluent membrane whorls undergo a more serious injury, resulting probably in an irreversible degeneration, which highly resembles the "dying back" (Spencer and Schaumburg 1975) or "watery-like" degeneration (Marques et al. 2003) types detailed above. However, in our model, dark processes are completely absent, at least, 3 days after the treatment.

Determination of the time point of our study and the relevance of our model

We have chosen 3-day-survival time because quantified Tph2 IR fiber density exhibited a significant reduction in parallel with the abundant appearance of swollen–fragmented axonal profiles 3 days after the treatment. In addition, previous studies on the electron microscopic characterization of amphetamine-caused axonal degeneration describe that both swollen and dark processes are highly abundant 2–3 days following drug treatment (Ryan et al. 1990).

In the Dark Agouti rat strain, the CYP2D1 enzyme, which is an important factor in MDMA metabolism and is the equivalent of the human CYP2D6 (debrisoquine hydroxylase), shows decreased activity. Thus, the metabolism of MDMA in these animals may be similarly reduced to vulnerable humans who exhibit decreased CYP2D6 activity (5–9% of Caucasian population), and might represent a genetically defined subpopulation in which acute clinical complications are more likely to occur when exposed to MDMA (de la Torre and Farre 2004; Malpass et al. 1999; Vorhees et al. 1999).

Comparative evaluation of light- and electron microscopic results and conclusion

In a recent paper, Wang et al. (2007) describes three potential models for studying the effect of MDMA on serotonergic nerve terminals. The "neuroadaptive" model posits that 5-HT terminals are intact after MDMA treatment although biochemical serotonergic parameters are reduced due to the persistent inhibition of serotonin synthesis. The "neurotoxic" model claims that some portion of serotonergic terminals is destroyed while other terminals are preserved. The "mixed" model states that some portion of serotonergic terminals is destroyed while others exhibit a neuroadaptive response.

In our study, the comparative analysis of light and electron microscopic results suggests that the light microscopic characteristic of Tph2 immunostaining in the frontal cortex 3 days after the treatment (reduced fiber density and swollen fragmented axonal profiles) may simultaneously reflect to the previously described reduction of the Tph enzyme expression (Bonkale and Austin 2008) and to the decreased axonal transport caused by the collapsed microtubular system. The fragmented-like morphology of serotonergic axons at light microscopic level, which is described by several previous studies, may reflect to the reduced axonal flow rather than the physical fragmentation of fibers.

Taken together, our results support the "mixed" hypothesis with further specification. In our model the most prominent serotonergic fiber alteration is the widespread microtubular destruction. According to our morphometric analysis, this alteration affects approximately 60% of all labeled serotonergic fibers in the frontal cortex (it should be considered that serotonergic fibers in which the level of Tph2 drops below the level of detectability are inherently unrecognizable.) However, most of these fibers with microtubular injury exhibit relatively well-preserved morphology of mitochondria. It is a question of debate, whether these fibers survive or degenerate later. It is interesting to note that aberrant swollen varicosities on Tph IR axons, which can be detected in a high amount 3 days after the MDMA treatment, disappear by 3 weeks while the quantified Tph IR axon density does not decrease further after 3 days (Adori, unpublished result). At the same time, a smaller portion of fibers with degenerated mitochondria and confluent membrane whorls observed in the present study probably undergo an irreversible degeneration. Since the degree of toxicity is known to be dose-related, a range of higher doses and longer survivals may contribute greatly to clarifying the ultrastructural changes related to toxic effect. Further ultrastructural analysis is required with the application of different doses of MDMA and sampling at several survival time intervals after the treatment to evaluate the proportion of intact, degenerating, and injured but surviving serotonergic axons more precisely to provide more details considering the damaging effects of MDMA administration on the serotonergic system of the brain.

Acknowledgement We are grateful to Katalin Komjáti, Ágnes Druskóné, Ildikó Csontos, and Mariann Lenkey for their excellent technical assistance. We also thank Dr. Katalin Gallatz and Dr. Lajos László for the invaluable discussion.

This study was supported by the 6th Framework Program of the European Community, LSHM-CT-2004-503474, the Hungarian Research Fund Grant T020500, the Ministry of Welfare Research Grant 460/2006, the Deutsche Forschungsgemeinschaft (SFB 581/B9, and SFB TRR 58/A1, A5) and TAMOP-4.2.1.B-09/1/KMR-2010.

References

Adori C, Ando RD, Kovacs GG, Bagdy G (2006) Damage of serotonergic axons and immunolocalization of Hsp27, Hsp72, and Hsp90 molecular chaperones after a single dose of MDMA administration in Dark Agouti rat: temporal, spatial, and cellular patterns. J Comp Neurol 497:251–269

Aguirre N, Barrionuevo M, Ramirez MJ, Del Rio J, Lasheras B (1999) Alpha-lipoic acid prevents 3, 4-methylenedioxy-methamphetamine (MDMA)-induced neurotoxicity. NeuroReport 10:3675–3680

Ando RD, Adori C, Kirilly E, Molnar E, Kovacs GG, Ferrington L, Kelly PA, Bagdy G (2010) Acute SSRI-induced anxiogenic and brain metabolic effects are attenuated 6 months after initial MDMA-induced depletion. Behav Brain Res 207:280–289

Arai R, Karasawa N, Kurokawa K, Kanai H, Horiike K, Ito A (2002) Differential subcellular location of mitochondria in rat serotonergic neurons depends on the presence and the absence of monoamine oxidase type B. Neuroscience 114:825–835

Baas PW, Qiang L (2005) Neuronal microtubules: when the MAP is the roadblock. Trends Cell Biol 15:183–187

Baker KG, Halliday GM, Tork I (1990) Cytoarchitecture of the human dorsal raphe nucleus. J Comp Neurol 301:147–161

Balogh B, Molnar E, Jakus R, Quate L, Olverman HJ, Kelly PA, Kantor S, Bagdy G (2004) Effects of a single dose of 3, 4-methylenedioxymethamphetamine on circadian patterns, motor activity and sleep in drug-naive rats and rats previously exposed to MDMA. Psychopharmacology (Berl) 173:296–309

Battaglia G, Yeh SY, De Souza EB (1988) MDMA-induced neurotoxicity: parameters of degeneration and recovery of brain serotonin neurons. Pharmacol Biochem Behav 29:269–274

Bellomo G, Mirabelli F, Vairetti M, Iosi F, Malorni W (1990) Cytoskeleton as a target in menadione-induced oxidative stress in cultured mammalian cells. I. Biochemical and immunocytochemical features. J Cell Physiol 143:118–128

Bendotti C, Baldessari S, Pende M, Tarizzo G, Miari A, Presti ML, Mennini T, Samanin R (1994) Does GFAP mRNA and mitochondrial benzodiazepine receptor binding detect serotonergic neuronal degeneration in rat? Brain Res Bull 34:389–394

Beveridge TJ, Mechan AO, Sprakes M, Pei Q, Zetterstrom TS, Green AR, Elliott JM (2004) Effect of 5-HT depletion by MDMA on hyperthermia and Arc mRNA induction in rat brain. Psychopharmacology (Berl) 173:346–352

Biezonski DK, Meyer JS (2010) Effects of 3, 4-methylenedioxymethamphetamine (MDMA) on serotonin transporter and vesicular monoamine transporter 2 protein and gene expression in rats: implications for MDMA neurotoxicity. J Neurochem 112:951–962

Bonkale WL, Austin MC (2008) 3, 4-Methylenedioxymethamphetamine induces differential regulation of tryptophan hydroxylase 2 protein and mRNA levels in the rat dorsal raphe nucleus. Neuroscience 155:270–276

Callahan BT, Cord BJ, Ricaurte GA (2001) Long-term impairment of anterograde axonal transport along fiber projections originating in the rostral raphe nuclei after treatment with fenfluramine or methylenedioxymethamphetamine. Synapse 40:113–121

Capela JP, Carmo H, Remiao F, Bastos ML, Meisel A, Carvalho F (2009) Molecular and cellular mechanisms of ecstasy-induced neurotoxicity: an overview. Mol Neurobiol 39:210–271

Chou SM, Hartmann HA (1964) Axonal lesions and waltzing syndrome after Idpn administration in rats. With a concept —"Axostasis". Acta Neuropathol 3:428–450

Cohen Z, Ehret M, Maitre M, Hamel E (1995) Ultrastructural analysis of tryptophan hydroxylase immunoreactive nerve terminals in the rat cerebral cortex and hippocampus: their associations with local blood vessels. Neuroscience 66:555–569

de la Torre R, Farre M (2004) Neurotoxicity of MDMA (ecstasy): the limitations of scaling from animals to humans. Trends Pharmacol Sci 25:505–508

De Repentigny Y, Deschenes-Furry J, Jasmin BJ, Kothary R (2003) Impaired fast axonal transport in neurons of the sciatic nerves from dystonia musculorum mice. J Neurochem 86:564–571

Fader CM, Colombo MI (2009) Autophagy and multivesicular bodies: two closely related partners. Cell Death Differ 16:70–78

Fischer C, Hatzidimitriou G, Wlos J, Katz J, Ricaurte G (1995) Reorganization of ascending 5-HT axon projections in animals previously exposed to the recreational drug (+/−)3, 4-methylenedioxymethamphetamine (MDMA, "ecstasy"). J Neurosci 15:5476–5485

Fornai F, Lenzi P, Frenzilli G, Gesi M, Ferrucci M, Lazzeri G, Biagioni F, Nigro M, Falleni A, Giusiani M, Pellegrini A, Blandini F, Ruggieri S, Paparelli A (2004) DNA damage and ubiquitinated neuronal inclusions in the substantia nigra and striatum of mice following MDMA (ecstasy). Psychopharmacology (Berl) 173:353–363

Fornai F, Soldani P, Lazzeri G, di Poggio AB, Biagioni F, Fulceri F, Batini S, Ruggieri S, Paparelli A (2005) Neuronal inclusions in degenerative disorders do they represent static features or a key to understand the dynamics of the disease? Brain Res Bull 65:275–290

Graham D, Lantos P (2002) Greenfield's neuropathology. Arnold publisher, London

Green AR, Mechan AO, Elliott JM, O'Shea E, Colado MI (2003) The pharmacology and clinical pharmacology of 3, 4-methylenedioxymethamphetamine (MDMA, "ecstasy"). Pharmacol Rev 55:463–508

Gutknecht L, Waider J, Kraft S, Kriegebaum C, Holtmann B, Reif A, Schmitt A, Lesch KP (2008) Deficiency of brain 5-HT synthesis but serotonergic neuron formation in Tph2 knockout mice. J Neural Transm 115:1127–1132

Gutknecht L, Kriegebaum C, Waider J, Schmitt A, Lesch KP (2009) Spatio-temporal expression of tryptophan hydroxylase isoforms in murine and human brain: convergent data from Tph2 knockout mice. Eur Neuropsychopharmacol 19:266–282

Holzel B, Pfister C (1981) Topography and cytoarchitecture of the raphe nuclei in the rat. J Hirnforsch 22:697–708

Joh TH, Shikimi T, Pickel VM, Reis DJ (1975) Brain tryptophan hydroxylase: purification of, production of antibodies to, and cellular and ultrastructural localization in serotonergic neurons of rat midbrain. Proc Natl Acad Sci USA 72:3575–3579

Kirilly E, Molnar E, Balogh B, Kantor S, Hansson SR, Palkovits M, Bagdy G (2008) Decrease in REM latency and changes in sleep quality parallel serotonergic damage and recovery after MDMA: a longitudinal study over 180 days. Int J Neuropsychopharmacol 11:795–809

Kivell B, Day D, Bosch P, Schenk S, Miller J (2010) MDMA causes a redistribution of serotonin transporter from the cell surface to the intracellular compartment by a mechanism independent of phospho-p38-mitogen activated protein kinase activation. Neuroscience 168:82–95

Kovacs GG, Ando RD, Adori C, Kirilly E, Benedek A, Palkovits M, Bagdy G (2007) Single dose of MDMA causes extensive decrement of serotoninergic fibre density without blockage of the fast axonal transport in Dark Agouti rat brain and spinal cord. Neuropathol Appl Neurobiol 33:193–203

Linder JC, Young SJ, Groves PM (1995) Electron microscopic evidence for neurotoxicity in the basal ganglia. Neurochem Int 26:195–202

Liposits Z, Gorcs T, Trombitas K (1985) Ultrastructural analysis of central serotoninergic neurons immunolabeled by silver-gold-intensified diaminobenzidine chromogen. Completion of immunocytochemistry with X-ray microanalysis. J Histochem Cytochem 33:604–610

Malek ZS, Dardente H, Pevet P, Raison S (2005) Tissue-specific expression of tryptophan hydroxylase mRNAs in the rat midbrain: anatomical evidence and daily profiles. Eur J Neurosci 22:895–901

Malpass A, White JM, Irvine RJ, Somogyi AA, Bochner F (1999) Acute toxicity of 3, 4-methylenedioxymethamphetamine (MDMA) in Sprague-Dawley and Dark Agouti rats. Pharmacol Biochem Behav 64:29–34

Marques SA, Taffarel M, Blanco Martinez AM (2003) Participation of neurofilament proteins in axonal dark degeneration of rat's optic nerves. Brain Res 969:1–13

Medana IM, Esiri MM (2003) Axonal damage: a key predictor of outcome in human CNS diseases. Brain 126:515–530

Meyer JS, Piper BJ, Vancollie VE (2008) Development and characterization of a novel animal model of intermittent MDMA ("Ecstasy") exposure during adolescence. Ann NY Acad Sci 1139:151–163

Molliver ME, Berger UV, Mamounas LA, Molliver DC, O'Hearn E, Wilson MA (1990) Neurotoxicity of MDMA and related compounds: anatomic studies. Ann NY Acad Sci 600:649–661, discussion 661-4

Mori S, Matsuura T, Takino T, Sano Y (1987) Light and electron microscopic immunohistochemical studies of serotonin nerve fibers in the substantia nigra of the rat, cat and monkey. Anat Embryol (Berl) 176:13–18

Morshedi MM, Rademacher DJ, Meredith GE (2009) Increased synapses in the medial prefrontal cortex are associated with repeated amphetamine administration. Synapse 63:126–135

Narciso MS, Hokoc JN, Martinez AM (2001) Watery and dark axons in Wallerian degeneration of the opossum's optic nerve: different patterns of cytoskeletal breakdown? An Acad Bras Cienc 73:231–243

Nixon RA, Cataldo AM (1995) The endosomal-lysosomal system of neurons: new roles. Trends Neurosci 18:489–496

O'Callaghan JP, Miller DB (1993) Quantification of reactive gliosis as an approach to neurotoxicity assessment. NIDA Res Monogr 136:188–212

O'Hearn E, Battaglia G, De Souza EB, Kuhar MJ, Molliver ME (1988) Methylenedioxyamphetamine (MDA) and methylenedioxymethamphetamine (MDMA) cause selective ablation of serotonergic axon terminals in forebrain: immunocytochemical evidence for neurotoxicity. J Neurosci 8:2788–2803

O'Shea E, Granados R, Esteban B, Colado MI, Green AR (1998) The relationship between the degree of neurodegeneration of rat brain 5-HT nerve terminals and the dose and frequency of administration of MDMA ('ecstasy'). Neuropharmacology 37:919–926

Orio L, O'Shea E, Sanchez V, Pradillo JM, Escobedo I, Camarero J, Moro MA, Green AR, Colado MI (2004) 3, 4-Methylenedioxymethamphetamine increases interleukin-1beta levels and activates microglia in rat brain: studies on the relationship with acute hyperthermia and 5-HT depletion. J Neurochem 89:1445–1453

WC PG (1986) The rat brain in stereotaxic coordinates, 2nd edn. Academic Press Inc., New York

Pickel VM, Joh TH, Reis DJ (1976) Monoamine-synthesizing enzymes in central dopaminergic, noradrenergic and serotonergic neurons. Immunocytochemical localization by light and electron microscopy. J Histochem Cytochem 24:792–306

Puerta E, Hervias I, Aguirre N (2009) On the mechanisms underlying 3, 4-methylenedioxymethamphetamine toxicity: the dilemma of the chicken and the egg. Neuropsychobiology 60:119–129

Quate L, McBean DE, Ritchie IM, Olverman HJ, Kelly PA (2004) Acute methylenedioxymethamphetamine administration: effects on local cerebral blood flow and glucose utilisation in the Dark Agouti rat. Psychopharmacology (Berl) 173:287–295

Ricaurte GA, Forno LS, Wilson MA, DeLanney LE, Irwin I, Molliver ME, Langston JW (1988) (+/−)3, 4-Methylenedioxymethamphetamine selectively damages central serotonergic neurons in nonhuman primates. JAMA 260:51–55

Rowland NE, Kalehua AN, Li BH, Semple-Rowland SL, Streit WJ (1993) Loss of serotonin uptake sites and immunoreactivity in rat cortex after dexfenfluramine occur without parallel glial cell reactions. Brain Res 624:35–43

Ryan LJ, Linder JC, Martone ME, Groves PM (1990) Histological and ultrastructural evidence that D-amphetamine causes degeneration in neostriatum and frontal cortex of rats. Brain Res 518:67–77

Sahenk Z, Mendell JR (1983) Studies on the morphologic alterations of axonal membraneous organelles in neurofilamentous neuropathies. Brain Res 268:239–247

Sharma HS, Kiyatkin EA (2009) Rapid morphological brain abnormalities during acute methamphetamine intoxication in the rat: an experimental study using light and electron microscopy. J Chem Neuroanat 37:18–32

Smiley JF, Goldman-Rakic PS (1996) Serotonergic axons in monkey prefrontal cerebral cortex synapse predominantly on interneurons as demonstrated by serial section electron microscopy. J Comp Neurol 367:431–443

Spencer PS, Schaumburg HH (1975) Nervous system dying-back disease produced by 2, 5-hexanedione. Trans Am Neurol Assoc 100:148–151

Tanner KD, Levine JD, Topp KS (1998) Microtubule disorientation and axonal swelling in unmyelinated sensory axons during vincristine-induced painful neuropathy in rat. J Comp Neurol 395:481–492

Tork I (1990) Anatomy of the serotonergic system. Ann NY Acad Sci 600:9–34, discussion 34-5

Vorhees CV, Morford LL, Inman SL, Reed TM, Schilling MA, Cappon GD, Moran MS, Nebert DW (1999) Genetic differences in spatial learning between Dark Agouti and Sprague-Dawley strains: possible correlation with the CYP2D2 polymorphism in rats treated neonatally with methamphetamine. Pharmacogenetics 9:171–181

Wang X, Baumann MH, Xu H, Rothman RB (2004) 3, 4-methylenedioxymethamphetamine (MDMA) administration to rats decreases brain tissue serotonin but not serotonin transporter protein and glial fibrillary acidic protein. Synapse 53:240–248

Wang X, Baumann MH, Dersch CM, Rothman RB (2007) Restoration of 3, 4-methylenedioxymethamphetamine-induced 5-HT depletion by the administration of L-5-hydroxytryptophan. Neuroscience 148:212–220

Weissmann D, Belin MF, Aguera M, Meunier C, Maitre M, Cash CD, Ehret M, Mandel P, Pujol JF (1987) Immunohistochemistry of tryptophan hydroxylase in the rat brain. Neuroscience 23:291–304

Welt K, Weiss J, Martin R, Dettmer D, Hermsdorf T, Asayama K, Meister S, Fitzl G (2004) Ultrastructural, immunohistochemical and biochemical investigations of the rat liver exposed to experimental diabetes und acute hypoxia with and without application of Ginkgo extract. Exp Toxicol Pathol 55:331–345